

A comparison of Hořava-Lifshitz gravity and Einstein gravity through thin-shell wormhole construction

F.Rahaman^{*}, P.K.F.Kuhfittig[†], M.Kalam[‡], A.A.Usmani[§] and Saibal Ray[¶]

^{*} Department of Mathematics, Jadavpur University, Kolkata - 700032, India

[†] Department of Mathematics, Milwaukee School of Engineering, Milwaukee, Wisconsin 53202-3109, USA

[‡] Department of Physics, Aliah University, Sector - V, Salt Lake, Kolkata - 700091, India

[§] Department of Physics, Aligarh Muslim University, Aligarh 202 002, Uttar Pradesh, India

[¶] Dept. of Physics, Govt. College of Engineering & Ceramic Technology, Kolkata 700 010, India

June 9, 2011

Abstract

In this paper we have constructed a new class of thin-shell wormholes from black holes in Hořava-Lifshitz gravity. Particular emphasis is placed on those aspects that allow a comparison of Hořava-Lifshitz to Einstein gravity. The former enjoys a number of advantages for small values of the throat radius.

PAC numbers: 04.40.Nr, 04.20.Jb, 04.20.Dw

1 Introduction

A new renormalizable gravity theory in four dimensions, proposed by Hořava [1], may be regarded as a UV complete candidate for general relativity. At large distances the theory reduces to Einstein gravity with a non-vanishing cosmological constant in IR, but with improved UV behavior. As discussed in Ref. [2], from the IR-modified Hořava action, which reduces to the standard Einstein-Hilbert action in the IR limit, one obtains the analogue of the standard spherically symmetric Schwarzschild-(A)dS black-hole solution.

In this paper we employ such a class of black holes by starting with two copies thereof and constructing a traversable thin-shell wormhole by means of the cut-and-paste technique [3]. To compare and contrast the two gravitational theories, we discuss various

^{*}farook_rahaman@yahoo.com

[†]kuhfitti@msoe.edu

[‡]mehedikalam@yahoo.co.in

[§]anisul@iucaa.ernet.in

[¶]saibal@iucaa.ernet.in

aspects of these wormholes, such as the location of the event horizons, the energy density of the thin shell, the violation of the weak energy condition at the junction surface, the amount of exotic matter required, and the equation of state. Our final topic is the question of stability to a linearized spherically symmetric perturbation.

2 Hořava-Lifshitz black holes

Consider the static and spherically symmetric line element

$$ds^2 = -N(r)^2 dt^2 + \frac{dr^2}{f(r)} + r^2(d\theta^2 + \sin^2\theta d\phi^2). \quad (1)$$

The modified Hořava action mentioned above is

$$\mathcal{L} = \frac{\kappa^2 \mu^2}{8(1-3\lambda)} \frac{N}{\sqrt{f}} \left[(2\lambda-1) \frac{(f-1)^2}{r^2} - 2\lambda \frac{f-1}{r} f' + \frac{\lambda-1}{2} f'^2 - 2(\omega - \Lambda_W)(1-f-rf') - 3\Lambda_W^2 r^2 \right], \quad (2)$$

where $\omega = 8\mu^2(3\lambda-1)/\kappa^2$ [4]. Here λ and κ are dimensionless coupling constants, while the constants μ and Λ_W are dimensionful.

The case $\lambda = 1$, which reduces to the standard Einstein-Hilbert action in the IR limit [2], yields

$$N^2 = f = 1 + (w - \Lambda_W)r^2 - \sqrt{r[w(w - 2\Lambda_W)r^3 + \gamma]}. \quad (3)$$

Here γ is an integration constant. By considering $\gamma = -\alpha^2/\Lambda_W$ and $\omega = 0$, this reduces to the solution given by Lu, Mei, and Pope (LMP) [5]:

$$f = 1 - \Lambda_W r^2 - \frac{\alpha}{\sqrt{-\Lambda_W}} \sqrt{r}. \quad (4)$$

If $\Lambda_W = 0$ and $\gamma = 4\omega M$ in Eq. (3), one obtains the Kehagias-Sfetsos (KS) black-hole solution [4]:

$$f = 1 + wr^2 - wr^2 \sqrt{1 + \frac{4M}{wr^3}}. \quad (5)$$

Finally, since $\lambda = 1$, we now have

$$\omega = \frac{16\mu^2}{\kappa^2}. \quad (6)$$

The Kehagias-Sfetsos solution is the only asymptotically flat solution in the family of solutions (3). We will therefore use the Kehagias-Sfetsos solution for constructing the thin-shell wormhole from Hořava-Lifshitz black holes. It is to be noted that there is an outer (event) horizon (r_+), and an inner (Cauchy) horizon (r_-) of the Kehagias-Sfetsos black-hole solution for $\omega M^2 > \frac{1}{2}$ at

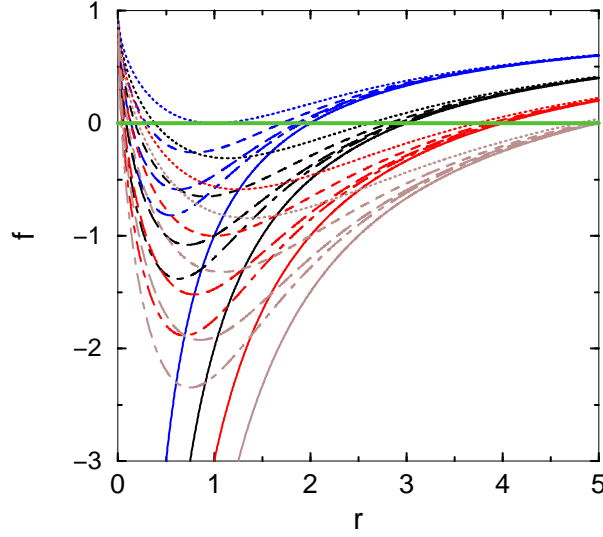


Figure 1: The plot for f using various parameters. The dotted, dashed, long dashed, and chain curves correspond to $\omega = 0.5, 1.0, 2.0$, and 3.0 , respectively. The thick solid lines corresponds to the Schwarzschild case. The blue, black, red and brown colors represent $M = 1.0, 1.5, 2.0$, and 2.5 , respectively.

$$r_{\pm} = M \left[1 \pm \sqrt{1 - \frac{1}{2wM^2}} \right], \quad (7)$$

compared to $\sqrt{1 - 2M/r}$ for the Schwarzschild case, i.e., in Einstein gravity.

This spacetime comes back to the Schwarzschild black hole for $r \gg (\frac{M}{w})^{1/3}$, so that

$$f \approx 1 - \frac{2M}{r} - \mathcal{O}(r^{-4}).$$

Finally, observe that

$$\begin{aligned} 0 = r_{-}(Schwarzschild) < r_{-}(KS) &= M \left[1 - \sqrt{1 - \frac{1}{2wM^2}} \right] \\ < r_{+}(KS) = M \left[1 + \sqrt{1 - \frac{1}{2wM^2}} \right] < 2M = r_{+}(Schwarzschild). \end{aligned} \quad (8)$$

The event horizons for various values of ω and their relationship to the Schwarzschild case can be seen in Fig. 1.

3 Thin-shell wormholes from Hořava-Lifshitz black holes

The mathematical construction of a thin-shell wormhole, when first proposed by Visser [27], used a flat Minkowski space as a starting point. The construction itself, however, relies on a topological identification of two surfaces and is not confined to a particular type of geometry. So we can safely start with two copies of a Kehagias-Sfetsos black hole and remove from each the four-dimensional region

$$\Omega^\pm = \{r \leq a \mid a > r_h\}.$$

We assume that $r_h = r_+$, the larger of the two radii. The construction proceeds by identifying (in the sense of topology) the timelike hypersurfaces

$$\partial\Omega^\pm = \{r = a \mid a > r_h\},$$

denoted by Σ . Thanks to the asymptotic flatness referred to above, the resulting manifold is geodesically complete and consists of two asymptotically flat regions connected by a throat, namely $r = a$.

Our main goal is to compare various characteristics of Hořava-Lifshitz gravity and Einstein gravity, such as the surface stress-energy tensor and the basic question of stability. A complete analysis would require, as always, a detailed knowledge of the junction conditions, but the traditional method, using the Lanczos equations, does not automatically carry over to Kehagias-Sfetsos black holes without an additional assumption. So let us return to Eq. (8) and Fig. 1, neither of which depends on the junction conditions, to gain an overview: the effect of the convergence to the Schwarzschild case can be clearly seen for the event horizons. But the convergence of the KS solution to the Schwarzschild solution is true in general and never depends on the junction conditions. From this standpoint, all well-constructed plots can be expected to show certain trends that allow a comparison between the two gravitational theories. Indeed, all the plots to follow show the gradual departure from the Schwarzschild limit as a decreases. The ability to make the relevant comparisons justifies the assumption that the thin-shell formalism is at least *qualitatively* acceptable, given that the use of plots is essentially qualitative in nature. For example, Fig. 7 shows that the amount of exotic matter required is *less* for the KS case than for the Schwarzschild case, which is indeed a qualitative statement. (This point will be reiterated from time to time when making the comparisons.)

A final observation in Fig. 1 is that the plot for f starts taking on a very different form from that of the Schwarzschild case for small values of $r = a$, enough to cast some doubt on the validity. This suspicion is readily confirmed by the fact that in some cases the results are actually unphysical for sufficiently small values of a ; such values may therefore be disregarded as meaningless.

With these caveats in mind, we will proceed with the assumption that the induced metric on Σ is given by

$$ds^2 = -d\tau^2 + a(\tau)^2(d\theta^2 + \sin^2\theta d\phi^2), \quad (9)$$

where τ is the proper time on the junction surface. It follows from the Lanczos equations [3, 6, 7, 8, 9, 10, 11, 12, 13, 14, 15, 16, 17, 18, 19, 20, 21, 22, 23, 24, 25, 26],

$$S^i_j = -\frac{1}{8\pi} ([K^i_j] - \delta^i_j [K]),$$

that the surface stress-energy tensor is $S^i_j = \text{diag}(-\sigma, p_\theta, p_\phi)$, where σ is the surface energy density and $p = p_\theta = p_\phi$ is the surface pressure. The Lanczos equations then yield

$$\sigma = -\frac{1}{4\pi} [K^\theta_\theta]$$

and

$$p = \frac{1}{8\pi} ([K^\tau_\tau] + [K^\theta_\theta]).$$

Following Ref. [3], a dynamic analysis can be obtained by letting the radius $r = a$ be a function of time. As a result,

$$\sigma = -\frac{1}{2\pi a} \sqrt{f(a) + \dot{a}^2} \quad (10)$$

and

$$p_\theta = p_\phi = p = -\frac{1}{2}\sigma + \frac{1}{8\pi} \frac{2\ddot{a} + f'(a)}{\sqrt{f(a) + \dot{a}^2}}, \quad (11)$$

where the overdot and prime denote, respectively, the derivatives with respect to τ and a . Here p and σ obey the conservation equation

$$\frac{d}{d\tau}(\sigma a^2) + p \frac{d}{d\tau}(a^2) = 0 \quad (12)$$

or

$$\dot{\sigma} + 2\frac{\dot{a}}{a}(p + \sigma) = 0. \quad (13)$$

For a static configuration of radius a , we need to assume that $\dot{a} = 0$ and $\ddot{a} = 0$. From Eqs. (10) and (11) we have

$$\sigma_{KS} = -\frac{1}{2\pi a} \sqrt{1 + wa^2 - wa^2 \sqrt{1 + \frac{4M}{wa^3}}} \quad (14)$$

in Hořava-Lifshitz gravity and

$$\sigma_{Schwarzschild} = -\frac{1}{2\pi a} \sqrt{1 - \frac{2M}{a}} \quad (15)$$

in Einstein gravity. Eq.(14) shows that the energy density of the shell is negative in the KS case, just as it is in the Schwarzschild case. We can see from Fig. 2 that in the KS case the energy density of the shell tends to be well below that of the Schwarzschild case, as long as a is not too small, which is a considerable advantage from the standpoint of wormhole design. As a gets large, however, σ_{KS} approaches $\sigma_{Schwarzschild}$, as expected

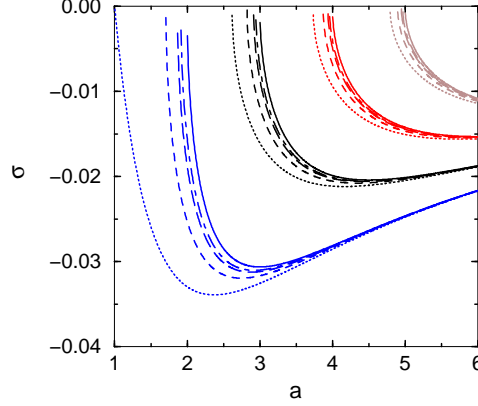


Figure 2: The plot for σ vs. a for various parameters. The description of the curves is the same as in Fig. 1.

from the discussion in Sec. 2. Qualitatively, Fig. 3 shows a similar advantageous behavior for the lateral pressure

$$p_{KS} = \frac{1}{8\pi} \left[\frac{4aw - 4aw\sqrt{1 + \frac{4M}{wa^3}} + \frac{6M}{a^2} \frac{1}{\sqrt{1 + 4M/wa^3}} + \frac{2}{a}}{\sqrt{1 + wa^2} - wa^2\sqrt{1 + \frac{4M}{wa^3}}} \right] \quad (16)$$

in Hořava-Lifshitz gravity and

$$p_{Schwarzschild} = \frac{1}{4\pi a} \left[\frac{1 - \frac{M}{a}}{\sqrt{1 - \frac{2M}{a}}} \right] \quad (17)$$

in Einstein gravity. Once again, the differences are greatest for somewhat smaller values of a . (Figs. 2 and 3 also show the effect of having different event horizons.)

Since the shell is infinitely thin, the radial pressure is zero. So the matter on the shell violates both the weak and null energy conditions.

4 Equation of state

Let us suppose that the EoS at the surface Σ is $p = W\sigma$, $W \equiv \text{constant}$. From Eqs. (14)-(17),

$$\frac{p_{KS}}{\sigma_{KS}} = W_{KS} = -\frac{a}{4} \left[\frac{4aw - 4aw\sqrt{1 + \frac{4M}{wa^3}} + \frac{6M}{a^2} \frac{1}{\sqrt{1 + 4M/wa^3}} + \frac{2}{a}}{1 + wa^2 - wa^2\sqrt{1 + \frac{4M}{wa^3}}} \right] \quad (18)$$

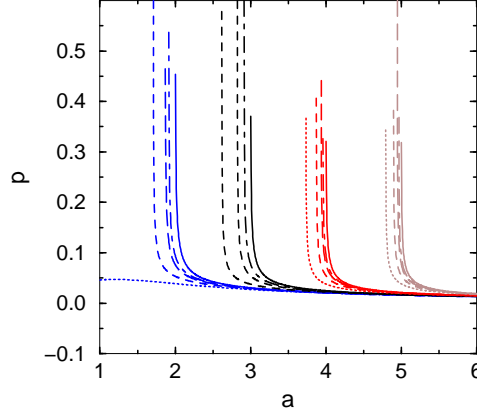


Figure 3: The plot for the pressure p vs. a for various parameters. The description of the curves is the same as in Fig. 1.

in Hořava-Lifshitz gravity and

$$\frac{p_{Schwarzschild}}{\sigma_{Schwarzschild}} = W_{Schwarzschild} = -\frac{1}{2} \left[\frac{1 - \frac{M}{a}}{1 - \frac{2M}{a}} \right] \quad (19)$$

in Einstein gravity. Even though $W_{KS} > W_{Schwarzschild}$, W_{KS} extends into the phantom-energy regime (less than -1), but in both cases, $W \rightarrow -1/2$ from below as $a \rightarrow \infty$, as shown in Fig. 4. The positive values are unphysical, corresponding to locations well inside the event horizon.

Another property worth checking is the traceless surface stress-energy tensor $S^i_i = 0$, i.e., $-\sigma + 2p = 0$. The reason is that the Casimir effect with a massless field is of the traceless type. From this equation we find that

$$C_{KS} \equiv 2 \left[1 + wa^2 - wa^2 \sqrt{1 + \frac{4M}{wa^3}} \right] + a \left[4aw - 4aw \sqrt{1 + \frac{4M}{wa^3}} + \frac{6M}{a^2} \frac{1}{\sqrt{1 + \frac{4M}{wa^3}}} + \frac{2}{a} \right] = 0 \quad (20)$$

in Hořava-Lifshitz gravity and

$$C_{Schwarzschild} \equiv 2 - \frac{3M}{a} = 0 \quad (21)$$

in Einstein gravity.

We can see from Fig. 5 that the values of a satisfying these equations lie inside the event horizon, ensuring that this situation cannot occur when dealing thin-shell worm-holes.

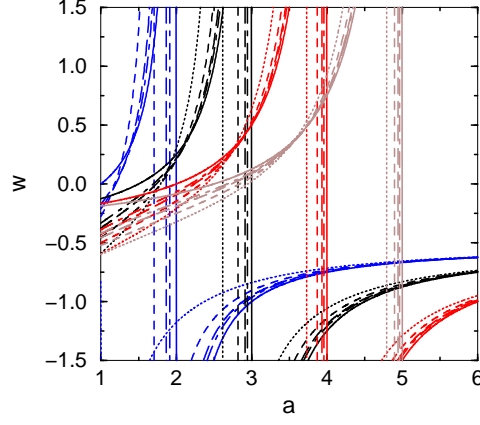


Figure 4: The plot for W vs. a for various parameters. The description of the curves is the same as in Fig. 1.

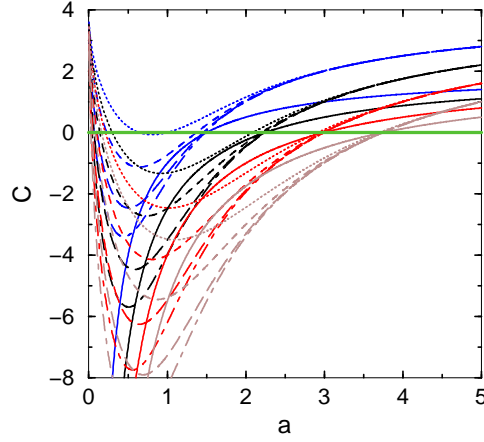


Figure 5: The curves C cut the a -axis at points less than the horizon (r_+). The description of the curves is the same as in Fig. 1.

5 The gravitational field

In this section we study the attractive or repulsive nature of our wormhole. To this end, we calculate the observer's four-acceleration

$$A^\mu = u^\mu_{;\nu} u^\nu,$$

where

$$u^\nu = \frac{dx^\nu}{d\tau} = \left(\frac{1}{\sqrt{f(r)}}, 0, 0, 0 \right).$$

It follows from Eq. (3) that the only nonzero component is given by

$$a^r = \Gamma_{tt}^r \left(\frac{dt}{d\tau} \right)^2 = \alpha(r),$$

where

$$\alpha(r)_{KS} = wr - wr \sqrt{1 + \frac{4M}{wr^3}} + \frac{3M}{r^2} \frac{1}{\sqrt{1 + \frac{4M}{wr^3}}} \quad (22)$$

in Hořava-Lifshitz gravity and

$$\alpha(r)_{Schwarzschild} = \frac{M}{r^2} \quad (23)$$

in Einstein gravity.

A test particle moving radially from rest obeys the geodesic equation

$$\frac{d^2 r}{d\tau^2} = -\Gamma_{tt}^r \left(\frac{dt}{d\tau} \right)^2 = -a^r.$$

It is true in general that a wormhole is attractive whenever $a^r > 0$ and repulsive whenever $a^r < 0$. According to Fig. 6, the wormholes are attractive in both gravitational theories, since the negative values in the KS case are well within the event horizon. Continuing the qualitative theme for small values of the throat radius, the acceleration is less for the KS case, which is an advantage for a traveler through the wormhole.

6 The total amount of exotic matter

An important consideration in wormhole physics is the total amount of exotic matter on the thin-shell. This total can be quantified by the integral [11, 12, 13, 14, 15, 16, 17]

$$\Omega_\sigma = \int [\rho + p] \sqrt{-g} d^3 x. \quad (24)$$

By introducing the radial coordinate $R = r - a$, we get

$$\Omega_\sigma = \int_0^{2\pi} \int_0^\pi \int_{-\infty}^\infty [\rho + p] \sqrt{-g} dR d\theta d\phi.$$

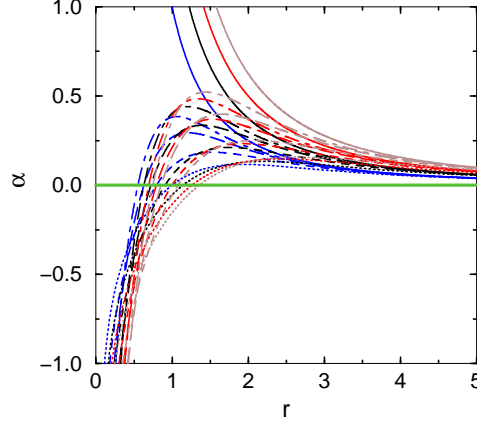


Figure 6: The plot for $\alpha(r)$ vs. a for various parameters. The description of the curves is the same as in Fig. 1.

Since the shell is infinitely thin, it does not exert any radial pressure, while $\rho = \delta(R)\sigma(a)$. So

$$\begin{aligned} \Omega_{\sigma \text{ KS}} &= \int_0^{2\pi} \int_0^\pi [\rho\sqrt{-g}]|_{r=a} d\theta d\phi = 4\pi a^2 \sigma(a) \\ &= -2a \sqrt{1 + wa^2} - wa^2 \sqrt{1 + \frac{4M}{wa^3}} \end{aligned} \quad (25)$$

in Hořava-Lifshitz gravity and

$$\Omega_{\sigma \text{ Schwarzschild}} = -2a \sqrt{1 - \frac{2M}{a}} \quad (26)$$

in Einstein gravity. According to Fig. 7, for small a the amount of exotic matter required is considerably less and may even be very much less for the KS than for the Schwarzschild case, which may be viewed as the most important difference between the two gravitational theories from the standpoint of wormhole design. (Once again, both Figs. 6 and 7 suggest that a must not be too small.)

7 Linearized stability

In this section we turn to the question of stability of the wormhole under small perturbations around a static solution $a = a_0$. It must be emphasized, however, that the analysis is subject to the same limitations already discussed in Sec. 3 and, as will be seen, clearly parallels our earlier findings.

Rearranging Eq. (10), we obtain the equation of motion of the thin shell:

$$\dot{a}^2 + V(a) = 0, \quad (27)$$

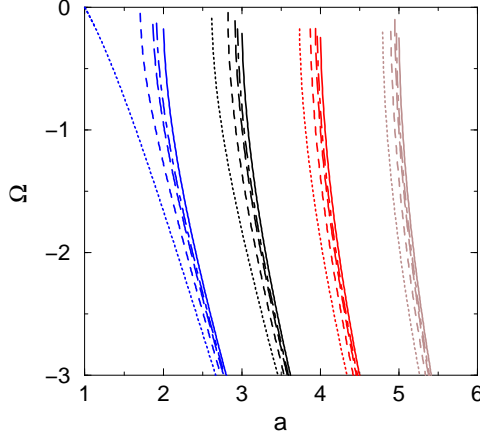


Figure 7: The plot for $\Omega_{\sigma \text{ KS}}$ and $\Omega_{\sigma \text{ Schwarzschild}}$ for various parameters. The description of the curves is the same as in Fig. 1.

where the potential $V(a)$ is defined as

$$V(a) = f(a) - [2\pi a\sigma(a)]^2. \quad (28)$$

Following Ref. [3], if we expand $V(a)$ around a_0 , we obtain

$$\begin{aligned} V(a) &= V(a_0) + V'(a_0)(a - a_0) + \frac{1}{2}V''(a_0)(a - a_0)^2 \\ &\quad + O[(a - a_0)^3], \end{aligned} \quad (29)$$

where the prime denotes the derivative with respect to a . Linearizing around $a = a_0$ requires that $V(a_0) = 0$ and $V'(a_0) = 0$. The configuration will be in stable equilibrium if $V''(a_0) > 0$. As suggested in Ref. [3], the subsequent analysis will make use of a parameter β , which is usually interpreted as the subluminal speed of sound and is given by the relation

$$\beta^2(\sigma) = \left. \frac{\partial p}{\partial \sigma} \right|_{\sigma}.$$

To determine the conditions that yield $V''(a_0) > 0$, it is convenient to start with Eq. (13) and first deduce that $(a\sigma)' = -(\sigma + 2p)$. Also,

$$(a\sigma)'' = -(\sigma' + 2p') = -\sigma' \left(1 + 2\frac{\partial p}{\partial \sigma} \right) = 2 \left(1 + 2\frac{\partial p}{\partial \sigma} \right) \frac{\sigma + p}{a} = 2(1 + 2\beta^2) \frac{\sigma + p}{a}. \quad (30)$$

Returning to Eq. (28), we now readily obtain

$$V'(a) = f'(a) + 8\pi^2 a\sigma(\sigma + 2p)$$

and

$$V''(a) = f''(a) - 8\pi^2(\sigma + 2p)^2 - 8\pi^2[2\sigma(1 + \beta^2)(\sigma + p)].$$

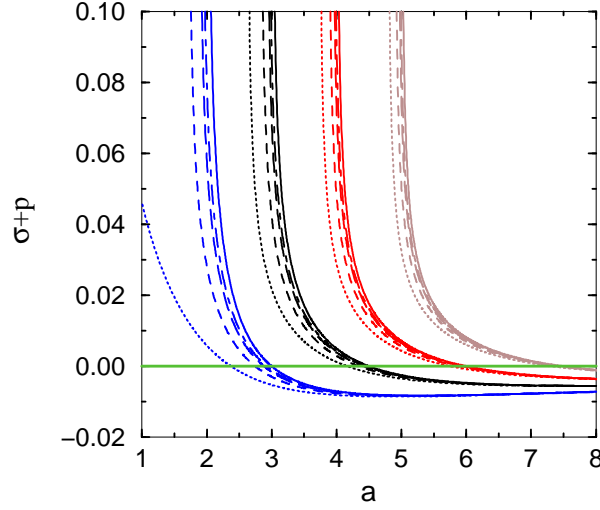


Figure 8: The plot for $\sigma + p$ vs. a for various parameters. The description of the curves is the same as in Fig. 1.

By direct computation we can now check the required conditions $V(a_0) = 0$ and $V'(a_0) = 0$. The stability condition $V''(a_0) > 0$ then yields the intermediate result

$$2\sigma(\sigma + p)(1 + 2\beta^2) < \frac{f''(a_0)}{8\pi^2} - (\sigma + 2p)^2. \quad (31)$$

Recall that σ is negative. If $\sigma + p$ is also negative, then the sense of the inequality is retained in the next step. If $\sigma + p$ is positive, then the sense of the inequality is reversed. (See Fig. 8.) In the former case we get

$$\beta^2 < \frac{\frac{f''(a_0)}{8\pi^2} - (\sigma + 2p)^2 - 2\sigma(\sigma + p)}{2[2\sigma(\sigma + p)]} \quad (32)$$

and in the latter case

$$\beta^2 > \frac{\frac{f''(a_0)}{8\pi^2} - (\sigma + 2p)^2 - 2\sigma(\sigma + p)}{2[2\sigma(\sigma + p)]}. \quad (33)$$

For these inequalities,

$$f(a_0) = 1 + wa_0^2 - wa_0^2 \sqrt{1 + \frac{4M}{wa_0^3}},$$

$$f'(a_0) = 2wa_0 - 2wa_0 \sqrt{1 + \frac{4M}{wa_0^3}} + \frac{6M}{a_0^2} \frac{1}{\sqrt{1 + \frac{4M}{wa_0^3}}},$$

and

$$f''(a_0) = 2w - 2w \sqrt{1 + \frac{4M}{wa_0^3}} + \frac{36M^2}{wa_0^6} \frac{1}{\left(1 + \frac{4M}{wa_0^3}\right)^{3/2}}$$

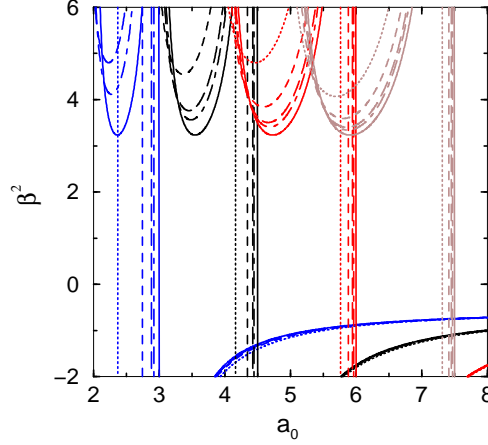


Figure 9: The plot for β^2 vs. a_0 for various parameters. The description of the curves is the same as in Fig. 1.

in the KS case and

$$f(a_0) = 1 - \frac{2M}{a_0},$$

$$f'(a_0) = \frac{2M}{a_0^2},$$

and

$$f''(a_0) = -\frac{4M}{a_0^3}$$

in the Schwarzschild case.

Fig. 9 shows the region of stability for both the KS and Schwarzschild cases. According to Eqs. (32) and (33) and Fig. 8, the respective regions of stability are below the curves on the right and above the curves on the left.

Under ordinary circumstances, β represents the velocity of sound, since $\beta^2 = \partial p / \partial \sigma$ is the square of the rate of change of distance with respect to time. So, ordinarily, $0 < \beta^2 \leq 1$. For the Schwarzschild case [3], the minimum value is $3/2 + \sqrt{3}$. According to Fig. 9, for the KS case, the region of stability involves values of β^2 that are even larger. (Of course, for the region on the right, β^2 is negative.) So by this criterion, there are no stable solutions for either type of wormhole.

All these interpretations are valid as long as β is indeed the speed of sound. As discussed extensively in Ref. [3], this assumption should be treated with caution when dealing with exotic matter. In this paper we have the additional complication that the KS case is based on a nonrelativistic gravitational theory. So we cannot exclude the possibility that β^2 is just a convenient parameter.

8 Conclusion

This paper discusses a new class of thin-shell wormholes from black holes in Hořava-Lifshitz gravity by employing the asymptotically flat Kehagias-Sfetsos (KS) solution with various values of the coupling constant ω and the mass M . In all cases the radius of the outer event horizon in the KS case turns out to be less than that in the Schwarzschild case. A wormhole designer from an advanced civilization would find several advantages in the KS case over the Schwarzschild case: for small values of the throat radius $r = a$, the negative energy density of the thin shell is well below that in the Schwarzschild case. The lateral pressure is also less. A particularly interesting finding is that for small values of a , the amount of exotic matter required can be much less for a KS than for a Schwarzschild wormhole, a considerable advantage given the problematical nature of exotic matter. As a gets large, however, the properties of the KS wormhole approach those of the Schwarzschild wormhole. A similar conclusion holds for the equation of state, assumed to be of the form $p = W\sigma$: while $W_{KS} > W_{Schwarzschild}$ for small a , in both gravitational theories $W \rightarrow -1/2$ as $a \rightarrow \infty$. While both types of wormholes are attractive, the acceleration toward the center is less for the KS case than for the Schwarzschild case, a particular advantage for a traveler. The final topic is a discussion of the stability to linearized radial perturbations in terms of a parameter β , normally interpreted as the speed of sound, but which may be just a convenient parameter. It was found that stable solutions exist in the KS case for values of β that are similar to the values in the Schwarzschild case.

Acknowledgment

FR is grateful for the financial support from UGC, Govt. of India.

References

- [1] P. Hořava, arXiv:0811.2217 [hep-th]; P. Hořava, JHEP **903**, 20 (2009) [arXiv:0812.4287 [hep-th]]; P. Hořava, Phys. Rev. D **79**, 084008 (2009) [arXiv:0901.3775 [hep-th]]; P. Hořava, arXiv:0902.3657 [hep-th].
- [2] Mu-in Park, JHEP **09**, 123 (2009).
- [3] E. Poisson and M. Visser, Phys. Rev. D **52**, 7318 (1995).
- [4] A. Kehagias and K. Sfetsos, Phys. Lett. B **678**, 123 (2009).
- [5] H. Lu, J. Mei and C. N. Pope, arXiv:0904.1595 [hep-th].
- [6] M. Visser, Nucl. Phys. B **328**, 203 (1989).
- [7] F.S.N. Lobo and P. Crawford, Class. Quant. Grav. **21**, 391 (2004).
- [8] F.S.N. Lobo, Class. Quant. Grav. **21**, 4811 (2004).

- [9] E.F. Eiroa and G. Romero, Gen. Rel. Grav. **36**, 651 (2004).
- [10] E.F. Eiroa and C. Simeone, Phys. Rev. D **70**, 044008 (2004).
- [11] E.F. Eiroa and C. Simeone, Phys. Rev. D **71**, 127501 (2005).
- [12] M. Thibeault, C. Simeone, and E.F. Eiroa, Gen. Rel. Grav. **38**, 1593 (2006).
- [13] F.S.N. Lobo, Phys. Rev. D **71**, 124022 (2005).
- [14] F. Rahaman et al., Gen. Rel. Grav. **38**, 1687 (2006).
- [15] E.F. Eiroa and C. Simeone, Phys. Rev. D **76**, 024021 (2007).
- [16] F. Rahaman et al., Int. J. Mod. Phys. D **16**, 1669 (2007).
- [17] F. Rahaman et al., Gen. Rel. Grav. **39**, 945 (2007).
- [18] F. Rahaman et al., Chin. J. Phys. **45**, 518 (2007) arXiv:0705.0740 [gr-qc]
- [19] M. G. Richarte and C. Simeone, Phys. Rev. D **76**, 087502 (2007).
- [20] J. P. S. Lemos and F.S.N. Lobo, Phys. Rev D **78**, 044030 (2008).
- [21] F. Rahaman et al., Acta Phys. Polon. B **40**, 1575 (2009) arXiv: gr-qc/0804.3852.
- [22] F. Rahaman et al., Mod. Phys. Lett. A **24**, 53 (2009) arXiv: gr-qc/0806.1391.
- [23] E.F. Eiroa, Phys. Rev. D **78**, 024018 (2008).
- [24] E.F. Eiroa, M.G. Richarte, and C. Simeone, Phys. Lett. A **373** 1 (2008).
- [25] F. Rahaman, K A Rahman, Sk.A Rakib, Peter K.F. Kuhfittig, Int. J. Theor. Phys. **49**, 2364 (2010). e-Print: arXiv:0909.1071 [gr-qc]
- [26] A.A. Usmani, Z. Hasan , F. Rahaman, Sk.A. Rakib, , Saibal Ray , Peter K.F. Kuhfittig, Gen. Relativ. Gravit. **42**, 2901 (2010) e-Print: arXiv:1001.1415 [gr-qc]
- [27] M. Visser, *Lorentzian wormholes—from Einstein to Hawking* (American Institute of Physics, New York, 1995).